Bulletin of Pure and Applied Sciences.

Vol. 38E (Math & Stat.), No.1, 2019. P.72-85 Print version ISSN 0970 6577 Online version ISSN 2320 3226

DOI: 10.5958/2320-3226.2019.00008.0

HEAT AND MASS TRANSFER ON MHD FLOW OF SECOND GRADE FLUID PAST A VERTICAL POROUS PLATE

B. Veera Sankar^{1,*} & B. Rama Bhupal Reddy²

Author Affiliation:

¹Research Scholar, Department of Mathematics, Rayalaseema University, Kurnool, Andhra Pradesh 518007, India

E-mail: veerasankar4@gmail.com

²Professor and Head, Department of Mathematics, KSRM College of Engineering, Kadapa, Andhra

Pradesh 516003, India E-mail: reddybrb@gmail.com

*Corresponding Author:

B. Veera Sankar, Research Scholar, Department of Mathematics, Rayalaseema University, Kurnool,

Andhra Pradesh 518007, India E-mail: veerasankar4@gmail.com

Received on 24.09.2018, Revised on 24.01.2019, Accepted on 25.02.2019

Abstract: In this paper, we discuss the magnetohydrodynamic (MHD) flow of second grade fluid through a loosely packed porous medium in an impulsively started vertical plate with variable heat and mass transfer. The temperature of plate is made to rise linearly with time. The fluid considered is gray, absorbing-emitting radiation but a non-scattering medium. The equations for the governing flow are solved by making use of the Laplace-transform technique. The velocity, temperature and concentration are obtained analytically and computationally discussed with reference to governing parameters and are illustrated graphically, and physical aspects of the problem are discussed. Also skin friction, Nusselt number and Sherwood number are obtained analytically and tabulated.

Keywords: Radiation effects, MHD flows, heat and mass transfer, vertical plates, porous medium, Skin friction, Nusselt number, Sherwood number.

2010 AMS Mathematics Subject Classification: 76E99, 76S05, 76S99, 76W99.

1. INTRODUCTION

Recent developments in contemporary technology have intensified the interest of many researchers towards the study of MHD flows through porous media on account of its extensive applications in geothermal and oil reservoir engineering as well as the erstwhile geophysical and astrophysical shove. The theoretical and experimental work on this subject can be found in the recent works of many authors, for example, Raptis [1] discussed unsteady free convection flow through a porous medium. Raptis and Perdikis [2] studied numerically free convection flow through a porous medium bounded by a semi-infinite vertical porous plate. Sattar [3] studied the same problem and obtained analytical solution by the perturbation technique adopted by Singh and Dikshit [4]. Recently, Krishna and Reddy M.G. [5] discussed MHD free convective rotating flow of viscoelastic fluid past an infinite vertical oscillating plate. Krishna and Reddy G.S. [6] discussed unsteady MHD convective flow of second grade fluid through a porous medium in a rotating parallel plate channel with temperature dependent source. Krishna and Swarnalathamma [7] discussed the peristaltic MHD flow of an

incompressible and electrically conducting Williamson fluid in a symmetric planar channel with heat and mass transfer under the effect of inclined magnetic field where, the viscous dissipation and Joule heating are also taken into consideration. Swarnalathamma and Krishna [8] discussed the theoretical and computational study of peristaltic hemodynamic flow of couple stress fluids through a porous medium under the influence of magnetic field with wall slip condition. Krishna D.V. et al. [9] discussed the unsteady hydromagnetic flow of an incompressible viscous fluid in a rotating parallel plate channel with porous lining under the influence of uniform transverse magnetic field normal to the channel and which work was extended by Krishna et al. [10]. Krishna et al. [11] studied the steady hydro magnetic flow of a couple stress fluid through a composite medium in a rotating parallel plate channel with porous bed on the lower half subjected to normal to the channel and extended the problem by taking the Hall current into account in a later work of Krishna et al. [12]. Krishna and Malashetty [13] discussed the unsteady flow of an incompressible electrically conducting second grade fluid in rigidly rotating parallel plate channel bounded below by a sparsely packed porous bed subjected to normal to the channel and further extended this problem by considering the Hall current in Krishna and Malashetty [14]. The effects of radiation and Hall current on an unsteady MHD free convective flow in a vertical channel filled with a porous medium have been studied by Veera Krishna et al. [15]. The heat generation/absorption and thermodiffusion on an unsteady free convective MHD flow of radiating and chemically reactive second grade fluid near an infinite vertical plate through a porous medium and taking the Hall current into account have been studied by Veera Krishna and Chamkha [16]. Veera Krishna et al. [18] discussed Hall effects on unsteady hydromagnetic natural convective rotating flow of second grade fluid past an impulsively moving vertical plate. In this paper, we consider radiation effects on MHD flow of second grade fluid past an impulsively started vertical porous plate with variable heat and mass transfer. The results are shown with the help of tables and graphs and an appendix and notations of the various symbols used are explained at the end of the paper.

2. FORMULATION AND SOLUTION OF THE PROBLEM

We consider the unsteady MHD flow of second grade fluid past an impulsively started vertical porous plate. The x- axis is taken along the plate in the upward direction and y-axis is taken normal to the plate. Initially the fluid and plate are at the same temperature. A transverse magnetic field B_0 of uniform strength is applied normal to the plate as shown in Figure 1. The viscous dissipation and induced magnetic field is neglected due to its small effect. Initially, the fluid and plate are at the same temperature T_1 and concentration C_1 in the stationary condition. At time t > 0, the plate is moving with a velocity $u = u_0$ in its own plane and the temperature of the plate is raised to T_w and the concentration level near the plate is raised linearly with respect to time.

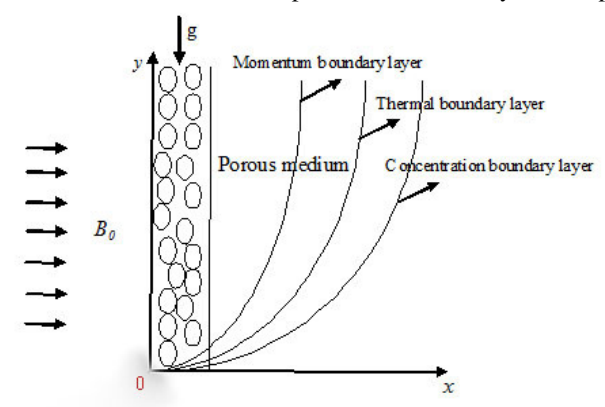


Figure 1: Physical configuration of the problem

The unsteady hydro magnetic equations of the MHD flow through porous medium are as:

$$\frac{\partial u}{\partial t} = v \frac{\partial^2 u}{\partial y^2} + \frac{\alpha_1}{\rho} \frac{\partial^3 u}{\partial y^2 \partial t} - \frac{\sigma_e B_0^2}{\rho} u - \frac{v}{K} u + g \beta (T - T_{\infty}) + g \beta^* (C - C_{\infty})$$
(1)

$$\rho C_p \frac{\partial T}{\partial t} = k \frac{\partial^2 T}{\partial y^2} - \frac{\partial q_r}{\partial y} \tag{2}$$

$$\frac{\partial C}{\partial t} = D_1 \frac{\partial^2 C}{\partial v^2} \tag{3}$$

The initial and boundary conditions

$$u = 0, T = T_{m}, C = C_{m}, \quad t \le 0, \quad \forall \quad y \tag{4}$$

$$u = u_0, T = T_{\infty} + (T_w - T_{\infty})At, C = C_{\infty} + (C_w - C_{\infty})At, \qquad y = 0$$
(5)

$$u \to 0, T \to T_{\infty}, C \to C_{\infty}, \quad y \to \infty$$
 (6)

where $A = \frac{u_0^2}{V}$, the local radiant for the case of an optically thin gray gas is expressed by

$$\frac{\partial q_r}{\partial y} = -4a^* \sigma (T_\infty^4 - T^4) \tag{7}$$

Considering the temperature difference within the flow sufficiently small, T^4 can be expressed as the linear function of temperature. This is accomplished by expanding T^4 in a Taylor series about T_∞ and neglecting higher-order terms, thus

$$T^4 \cong 4T_{\infty}^3 T - 3T_{\infty}^4 \tag{8}$$

Using equations (7) and (8), equation (2) reduces to

$$\rho C_p \frac{\partial T}{\partial t} = k \frac{\partial^2 T}{\partial y^2} + 16a^* \sigma (T_\infty^3 - T^4)$$
(9)

Introducing the following non-dimensional quantities:

$$u^* = \frac{u}{u_0}, \ y^* = \frac{yu_0}{v}, \ \theta = \frac{T - T_{\infty}}{T_w - T_{\infty}}, \ C^* = \frac{C - C_{\infty}}{C_w - C_{\infty}}, \ \mu = \rho v, \ t^* = \frac{tu_0^2}{v}$$

Making use of non-dimensional variables, the equations (1), (2) and (9) leads to (dropping asterisks)

$$\frac{\partial u}{\partial t} = \frac{\partial^2 u}{\partial y^2} + \alpha \frac{\partial^3 u}{\partial y^2 \partial t} - \left(M^2 + \frac{1}{D} \right) u + \operatorname{Gr} \theta + \operatorname{Gm} C$$
(10)

$$\frac{\partial \theta}{\partial t} = \frac{1}{\Pr} \frac{\partial^2 \theta}{\partial y^2} - \frac{R}{\Pr} \theta \tag{11}$$

$$\frac{\partial C}{\partial t} = \frac{1}{Sc} \frac{\partial^2 C}{\partial y^2} \tag{12}$$

with the boundary conditions

$$u = 0, \theta = 0, C = 0, \quad t \le 0, \quad \forall y$$
 (13)

$$u = 1, \ \theta = t, C = t, \qquad y = 0 \tag{14}$$

$$u \to 0, \theta \to 0, C \to 0, as \quad y \to \infty$$
 (15)

where, $R = \frac{16a^*v^2\sigma T_{\infty}^3}{ku_0^2}$ is the Radiation parameter, $M^2 = \frac{\sigma_e B_0^2 v}{\rho u_0^2}$ is the Hartmann number, $D = \frac{Ku_0^2}{v^2}$ is

the Darcy parameter, $Gr = \frac{g\beta v(T_w - T_\infty)}{u_0^3}$ is the thermal Grashof number, $Gm = \frac{g\beta^* v(C_w - C_\infty)}{u_0^3}$ the

mass Grashof number, $\Pr = \frac{\mu C_p}{k}$ is Prandtl parameter, $\alpha = \frac{\alpha_j u_0^2}{\rho v^2}$ is the second grade fluid parameter and

$$Sc = \frac{v}{D_1}$$
 is the Schmidt number.

The dimensionless governing equations (10) to (12), subject to the boundary conditions (13) to (15), are solved by the usual Laplace transform technique. Transforming equation (12) we get,

$$s\overline{C}(y,s) - C(y,0) = \frac{1}{Sc} \frac{d^2\overline{C}}{dy^2}$$
 (16)

Using boundary conditions (13) to (15), we have,

$$\frac{d^2\overline{C}}{dy^2} - s\,Sc\,\overline{C}(y,s) = 0\tag{17}$$

The solution of the equation (16) is

$$\overline{C}(y,s) = Ae^{\sqrt{sSc}y} + Be^{-\sqrt{sSc}y}$$
(18)

where A and B are arbitrary constants.

Again using the above boundary conditions (13) and (14), we get,

$$\overline{C}(y,s) = \frac{1}{s^2} e^{-\sqrt{sS_{C}y}}$$
(19)

Taking the inverse Laplace transform for the equation (19) yields,

$$C(y,t) = t \left(1 + 2\left(\frac{y}{2\sqrt{t}}\right)^2 Sc \right) erfc\left(\left(\frac{y}{2\sqrt{t}}\right)\sqrt{Sc}\right) - \frac{2\left(\frac{y}{2\sqrt{t}}\right)\sqrt{Sc}}{\sqrt{\pi}} e^{-\left(\frac{y}{2\sqrt{t}}\right)^2 Sc}$$
(20)

Also transforming the equation (11) renders

$$s\overline{\theta}(y,s) - \theta(y,0) = \frac{1}{\Pr} \frac{d^2\overline{\theta}}{dy^2} - \frac{R}{\Pr} \overline{\theta}(y,s)$$
 (21)

Using the boundary conditions (13) and (14), it reduces to:

$$\frac{d^2\overline{\theta}}{dy^2} - (R + s \operatorname{Pr})\overline{\theta}(y, s) = 0$$
(22)

The solution to this equation (21) is

$$\overline{\theta}(y,s) = C e^{y\sqrt{R+sPr}} + E e^{-y\sqrt{R+sPr}}$$
(23)

where, C and E are arbitrary constants. The values of C and E can be computed by using (13) and (14) to give

$$\overline{\theta}(y,s) = \frac{1}{s^2} e^{-y\sqrt{\Pr\left(s + \frac{R}{\Pr}\right)}}$$
(24)

Taking now the inverse Laplace transform for the equation (23), we obtain

$$\theta(y,t) = \frac{t}{2} \left(a_1 e^{2\xi\sqrt{Rt}} \operatorname{erfc}(\xi\sqrt{\Pr} + \sqrt{ct}) + a_2 e^{-2\xi\sqrt{Rt}} \operatorname{erfc}(\xi\sqrt{\Pr} - \sqrt{ct}) \right)$$
(25)

Similarly, again taking the Laplace transform of the equation (10) and making use of the initial and boundary conditions (13) to (15), it reduces to

$$(1+s\alpha)\frac{d^2u}{dy^2} - \left[s + \left(M^2 + \frac{1}{D}\right)\right] - \operatorname{Gr}L\{\theta(y,t)\} - \operatorname{Gm}L\{C(y,t)\}$$
(26)

The solution of the equation (26) is

$$\frac{1}{u(y,s)} = F e^{y\sqrt{\frac{s+(M^2+\frac{1}{D})}{1+s\alpha}}} + G e^{-y\sqrt{\frac{s+(M^2+\frac{1}{D})}{1+s\alpha}}} + \frac{Gr}{(1-Pr)(1+s\alpha)} e^{-y\sqrt{Pr}\sqrt{s+\frac{R}{Pr}}} + \frac{Gm}{(1-Sc)(1+s\alpha)} e^{-y\sqrt{sSc}} + \frac{e^{-y\sqrt{sSc}}}{s^2(s-a_4)}$$
(27)

Applying the boundary conditions (13) and (14) for (26), we obtain

$$\frac{1}{u(y,s)} = \frac{1}{s} e^{-y\sqrt{\frac{s+\left(M^2 + \frac{1}{D}\right)}{1+s\alpha}}} + \frac{Gr}{1-Pr} \left(\frac{e^{-y\sqrt{Pr}\sqrt{s+\frac{R}{Pr}}} - e^{-y\sqrt{\frac{s+\left(M^2 + \frac{1}{D}\right)}{1+s\alpha}}}}{s^2(s-a_3)(1+s\alpha)}\right) + \frac{Gm}{1-Sc} \left(\frac{e^{-y\sqrt{sSc}} - e^{-y\sqrt{\frac{s+\left(M^2 + \frac{1}{D}\right)}{1+s\alpha}}}}{s^2(s-a_4)(1+s\alpha)}\right)$$
(28)

Taking the inverse Laplace transform of the equation (28), we obtain the velocity as

$$\begin{split} u(y,t) &= a_{5} \ e^{-y\sqrt{\left(M^{2} + \frac{l}{D}\right)}} \ erfc \left(\xi - \sqrt{\left(M^{2} + \frac{l}{D}\right)t}\right) \\ &+ a_{6} \ e^{y\sqrt{\left(M^{2} + \frac{l}{D}\right)}} \ erfc \left(\xi + \sqrt{\left(M^{2} + \frac{l}{D}\right)t}\right) + \\ &- \left[e^{-y\sqrt{\Pr(a_{s} + (R/\Pr))}} \ erfc \left(\xi\sqrt{\Pr} - \sqrt{(a_{3} + (R/\Pr))t}\right) + \\ &e^{y\sqrt{\Pr(a_{s} + (R/\Pr))}} \ erfc \left(\xi\sqrt{\Pr} + \sqrt{(a_{3} + (R/\Pr))t}\right) \right] \ \frac{a_{11}}{2} e^{a_{s}t} \\ &- \left[e^{-y\sqrt{\Pr(a_{s} + (R/\Pr))}} \ erfc \left(\xi\sqrt{\Pr} - \sqrt{(-(1/\alpha) + (R/\Pr))t}\right) + \\ &e^{y\sqrt{\Pr(-(1/\alpha) + (R/\Pr))}} \ erfc \left(\xi\sqrt{\Pr} - \sqrt{(-(1/\alpha) + (R/\Pr))t}\right) \right] \ \frac{a_{11}}{2} e^{-(1/\alpha)t} \\ &- \left(a_{7} e^{-y\sqrt{\Pr(R/\Pr)}} \ erfc \left(\xi\sqrt{\Pr} - \sqrt{(R/\Pr)t}\right) + a_{8} e^{y\sqrt{\Pr(R/\Pr)}} \ erfc \left(\xi\sqrt{\Pr} + \sqrt{(R/\Pr)t}\right) \right) \\ &- \left[e^{-y\sqrt{\Pr\left(M^{2} + \frac{l}{D} + a_{3}\right)}} \ erfc \left(\xi\sqrt{\Pr} - \sqrt{\Pr\left(M^{2} + \frac{l}{D} + a_{3}\right)t}\right) + \\ &e^{y\sqrt{\Pr\left(M^{2} + \frac{l}{D} + a_{3}\right)}} \ erfc \left(\xi\sqrt{\Pr} - \sqrt{\Pr\left(M^{2} + \frac{l}{D} + a_{3}\right)t}\right) \right] \ \frac{a_{11}}{2} e^{a_{s}t} \\ &- \left[e^{-y\sqrt{\Pr\left(M^{2} + \frac{l}{D} + a_{3}\right)}} \ erfc \left(\xi\sqrt{\Pr} - \sqrt{\Pr\left(M^{2} + \frac{l}{D} + a_{3}\right)t}\right) \right] \ \frac{a_{11}}{2} e^{a_{s}t} \\ &+ \left[e^{-y\sqrt{a_{s}N_{c}}} \ erfc \left(\xi\sqrt{N_{c}} - \sqrt{a_{s}t}\right) + e^{y\sqrt{a_{s}N_{c}}} \ erfc \left(\xi\sqrt{N_{c}} + \sqrt{a_{s}t}\right) \right] \frac{a_{11}}{2} e^{-(1/\alpha)t} \\ &+ \left[e^{-y\sqrt{a_{s}N_{c}}} \ erfc \left(\xi\sqrt{N_{c}} - \sqrt{a_{s}t}\right) + e^{y\sqrt{a_{s}N_{c}}} \ erfc \left(\xi\sqrt{N_{c}} + \sqrt{a_{s}t}\right) \right] \frac{a_{12}}{2} e^{a_{s}t} \end{aligned}$$

$$+\left[e^{-y\sqrt{-(1/\alpha)Sc}} \ erfc \left(\xi\sqrt{Sc} - \sqrt{-(1/\alpha)t}\right) + e^{y\sqrt{a_{s}Sc}} \ erfc \left(\xi\sqrt{Sc} + \sqrt{-(1/\alpha)t}\right)\right] \frac{a_{12}}{2} e^{-(1/\alpha)t}$$

$$-\left[e^{-y\sqrt{\frac{M^{2} + \frac{1}{D} + a_{4}}{1 + a_{4}\alpha}}}\right] erfc \left(\xi - \sqrt{\frac{M^{2} + \frac{1}{D} + a_{4}}{1 + a_{4}\alpha}}\right)t\right] + e^{y\sqrt{\frac{M^{2} + \frac{1}{D} + a_{4}}{1 + a_{4}\alpha}}} erfc \left(\xi + \sqrt{\frac{M^{2} + \frac{1}{D} + a_{4}}{1 + a_{4}\alpha}}\right)t\right] \frac{a_{12}}{2} e^{a_{s}t}$$

$$-\left[e^{-y\sqrt{M^{2} + \frac{1}{D} - \frac{1}{\alpha}}} erfc \left(\xi - \sqrt{M^{2} + \frac{1}{D} - \frac{1}{\alpha}}\right)t\right] + e^{y\sqrt{\frac{M^{2} + \frac{1}{D} - \frac{1}{\alpha}}{\alpha}}} erfc \left(\xi + \sqrt{M^{2} + \frac{1}{D} - \frac{1}{\alpha}}t\right)\right] \frac{a_{12}}{2} e^{-(1/\alpha)t}$$

$$-a_{12}\left[1 + a_{4}t(1 + 2\xi^{2}Sc)erfc(\xi\sqrt{Sc}) + \frac{2a_{4}t\xi\sqrt{Sc}}{\sqrt{\pi}}e^{-\xi^{2}Sc}\right]$$

$$(29)$$

The non-dimensional shear stress is given by

$$\tau = -\left(\frac{du}{dy}\right)_{y=0} = -\frac{1}{2\sqrt{t}} \left(\frac{du}{d\xi}\right)_{\xi=0} \tag{30}$$

The non-dimensional Nusselt number is given by

$$Nu = -\left(\frac{d\theta}{dy}\right)_{y=0} = -\frac{1}{2\sqrt{t}} \left(\frac{d\theta}{d\xi}\right)_{\xi=0}$$
(31)

The non-dimensional Sherwood number is given by

$$Sh = -\left(\frac{dC}{dy}\right)_{y=0} = -\frac{1}{2\sqrt{t}} \left(\frac{dC}{d\xi}\right)_{\xi=0} \tag{32}$$

3. RESULTS AND DISCUSSION

We now discuss the exact analysis and present the investigation of the combined effects of heat and mass transfer on the MHD flow of second grade fluid bounded by loosely packed porous medium in an impulsively started vertical plate with variable heat and mass transfer. The expressions for the velocity, temperature and concentration are obtained by using the Laplace transform technique and we also discuss the physical behavior of the dimensionless parameters such as the Hartmann number M, the Darcy parameter D (Permeability parameter), the Radiation parameter R, α the visco-elastic parameter, the thermal Grashoff number Gr, the mass Grashoff number Gm, the Prandtl number Pr and the Schmidt number Sc. Figures 2-13 display the velocity, temperature and concentration. The Skin friction, Nusselt number and Sherwood number are shown in Tables (1-3). The velocity, temperature and concentration profiles for some realistic values of the Prandtl number Pr (Pr = 0.71, 0.16, 3 for the saturated liquid Freon at 273.3° and Pr = 7 for water) and the Schmidt number Sc (Sc = 0.2 for hydrogen) respectively. From figure 2, which shows the velocity profile for different values of M other parameters being fixed, we notice that the velocity decreases with increasing Hartmann number M. This is due to the fact that the application of transverse magnetic field results in a resistive type force (Lorentz force) similar to the drag force and upon increasing the intensity of the magnetic field which leads to the deceleration of the flow. Figure 3 is sketched in order to explore the variations of permeability parameter D. It is found that the magnitude of the velocity increases with increasing the values of permeability parameter D. This is due to the fact that increasing the permeability reduces the drag force which considerably assists the fluid to move fast. Likewise the magnitude of the velocity u reduces continuously with the increasing radiation parameter R as is evident from Figure 4. The magnitude of the velocity enhances with increasing second grade parameter α (see, Fig. 5). The variation of velocity for different values of dimensionless time t and Prandtl number Pr is shown in the Figures 6 and 7. It is noticed that the velocity increases with increasing time t. It is also observed from the Figure 7 that the magnitude of the velocity u decreases with increasing Prandtl number Pr. It is clear from the Figure 8 that the velocity decreases with increasing thermal Grashof number Gr (cooling plate), where as there is a sharp enhancement in the velocity on heating the plate, this is increase sustains away from the plate. Figure 9 reveals that the magnitude of the velocity increases with increasing mass Grashoff number Gm throughout the fluid region. Similarly the same phenomenon is observed with increasing Schmidt number Sc from Figure 10. The effect of radiation parameter R on the temperature profile is shown in Figure 11. It is inferred that the temperatures, being as decreasing function of R, decelerates the fluid flow and reduces the fluid velocity. Such an effect may also be expected here as the increasing radiation parameter R makes the fluid thick and ultimately causes the temperature and thermal boundary layer thickness to reduce. Hence it is observed that the temperature decreases with increasing radiation parameter R throughout the fluid region. The Prandtl number actually describes the relationship between momentum diffusivity and thermal diffusivity and hence controls the relative thickness of the momentum and thermal boundary layers. From Figure 12, we observe that the temperature reduces with increasing values of Prandtl number Pr, it is also observed that the thermal boundary layer thickness is maximum near the plate and reduces with increasing distances from the leading edge and finally approaches to zero. It is also justified due to the fact that thermal conductivity of the fluid decreases with increasing Prandtl number Pr and hence decreases the thermal boundary layer and the temperature profile. Figure 13 depicts that the increasing values of Schmidt number Sc leads to fall in the concentration profiles throughout the fluid.

The numerical values of the skin friction (τ) , Nusselt number (Nu) and Sherwood number (Sh) are computed and are tabulated in the Tables 1-3, in all these tables the comparison of each parameter is made with the first row in the corresponding table. It is found from the Table 1 that the effect of each parameter on the skin friction shows that τ increases with increasing R, D, α , Pr, Gr, Gm, Sc and time t, while decreases with M and -Gr. It is also readily seen from the Table 2 that the Nusselt number Nu increases with increasing R, Pr and t and from the Table 3 we observe that the Sherwood number goes on increasing with increasing Sc and t.

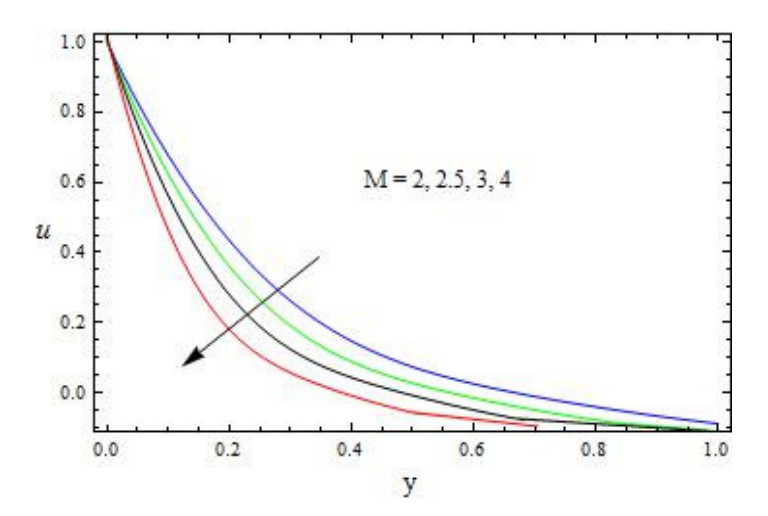


Figure 2: The velocity Profile for u against M with $\alpha = 1$; D=1; P= 0.71; t=0.1; Sc=2; R=1; Gr=5; Gm=10

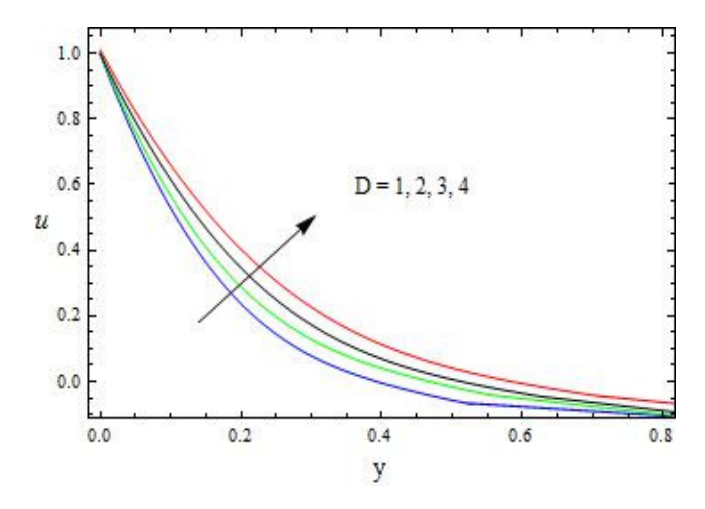


Figure 3: The velocity Profile for u against D with $\alpha = 1$; M=2; P= 0.71; t=0.1; Sc=2; R=1; Gr=5; Gm=10

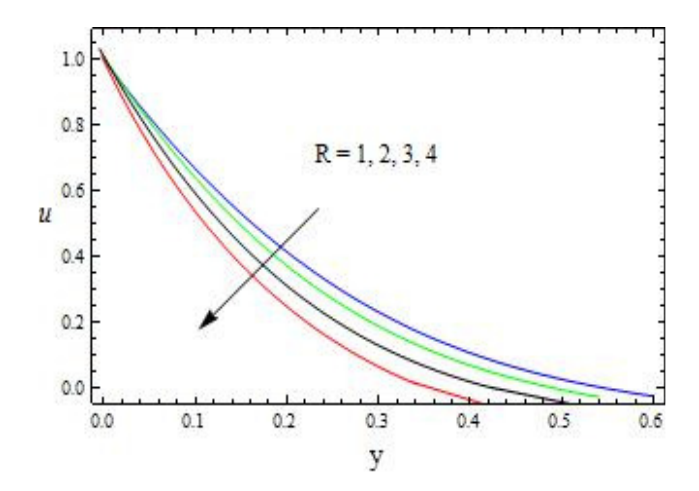


Figure 4: The velocity Profile for u against R with $\alpha = 1$; D=1; P= 0.71; t=0.1; Sc=2; M=2; Gr=5; Gm=10

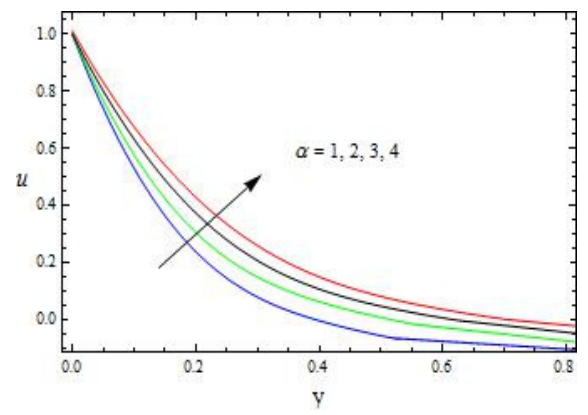


Figure 5: The velocity Profile for u against α with D=1; P= 0.71; t=0.1; R=1; Sc=2; M=2; Gr=5; Gm=10

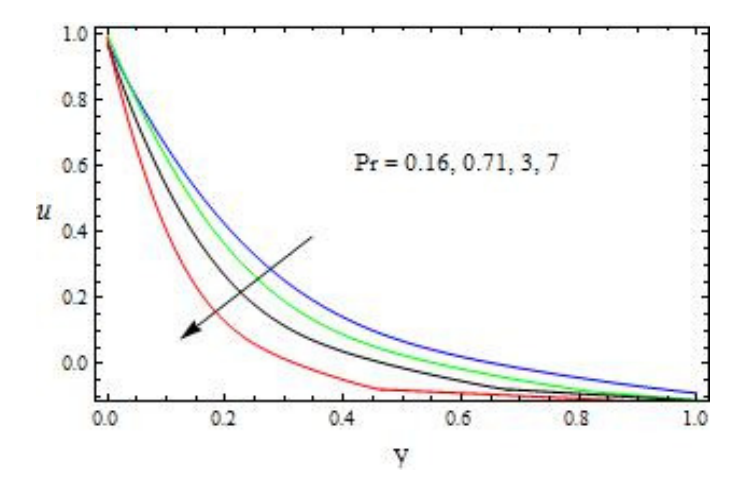


Figure 6: The velocity Profile for u against Pr and t with α = 1; M=2; D=1; t=0.1; Sc=2; R=1; Gr=5; Gm=10

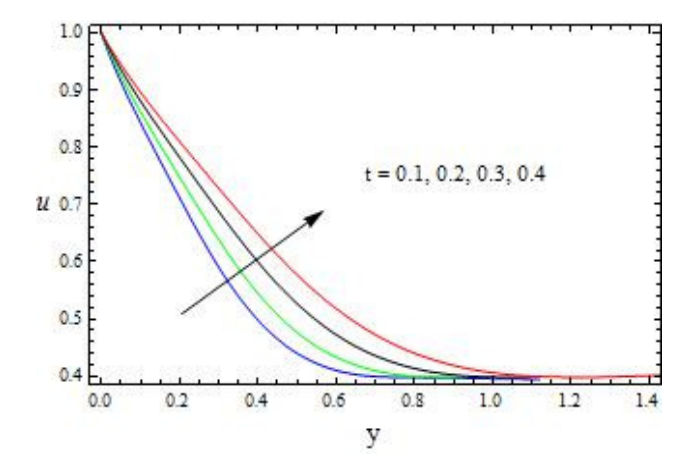


Figure 7: The velocity Profile for u against t with $\alpha = 1$; M=2; D=1; t=0.1; Sc=2; R=1; Gr=5; Gm=10

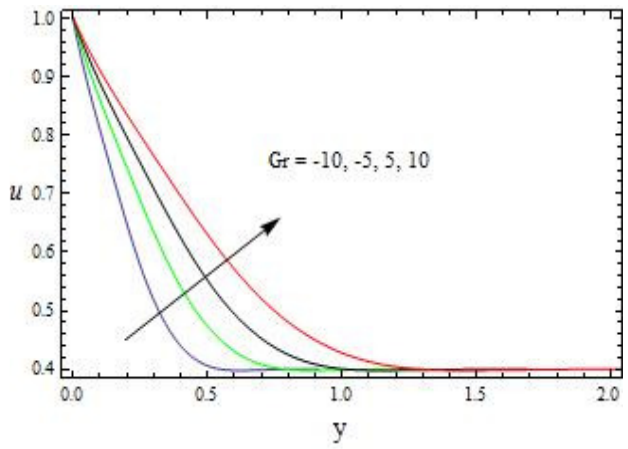


Figure 8: The velocity Profile for u against Gr with $\alpha = 1$; M=2; D=1; P=0.71; Sc=2; R=1; t=0.1; Gm=10

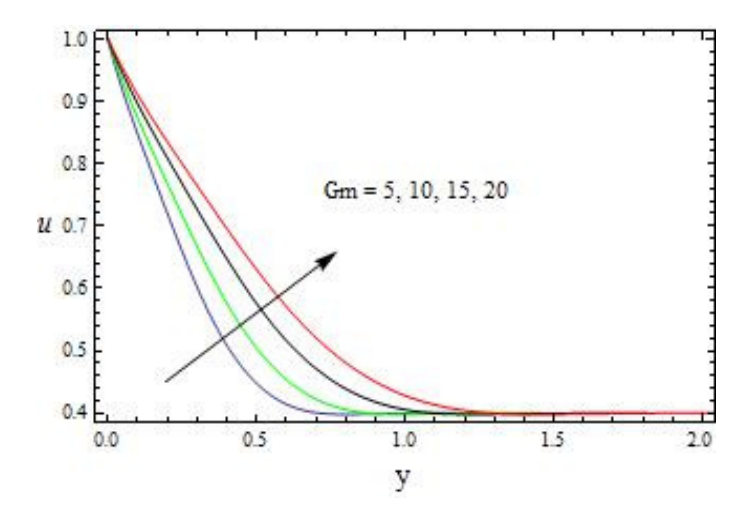


Figure 9: The velocity Profile for u against Gm with $\alpha = 1$; M=2; D=1; P=0.71, Sc=2; R=1; t=0.1; Gr=5

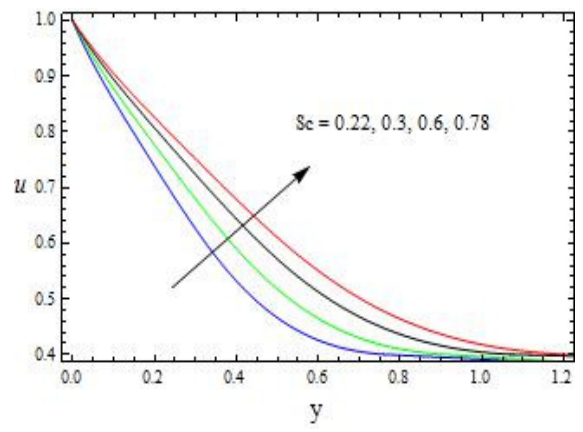


Figure 10: The velocity Profile for u against Sc with $\alpha = 1$; M=2; D=1; P=0.71, R=1; t=0.1; Gr=5; Gm=10

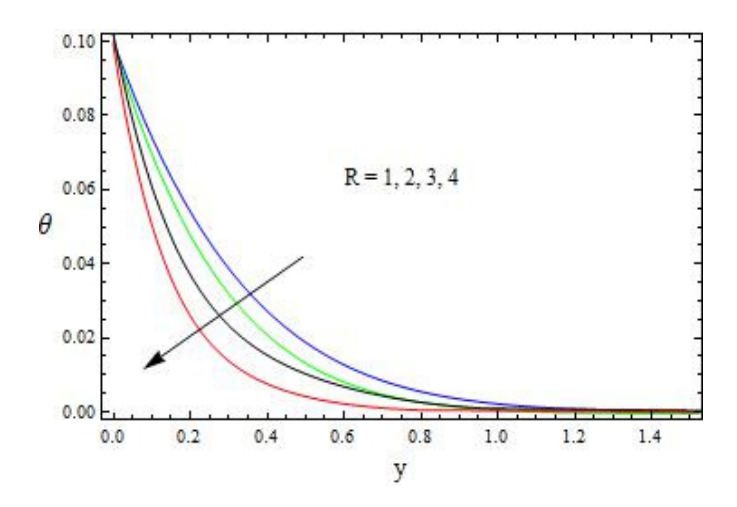


Figure 11: The Temperature Profile for θ against R with P=0.71; t=0.1

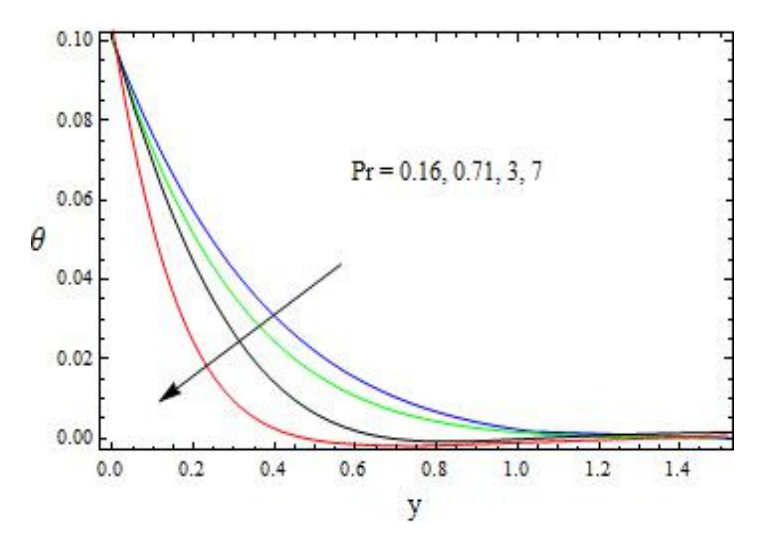


Figure 12: The Temperature Profile for θ against Pr with R=2; t=0.1

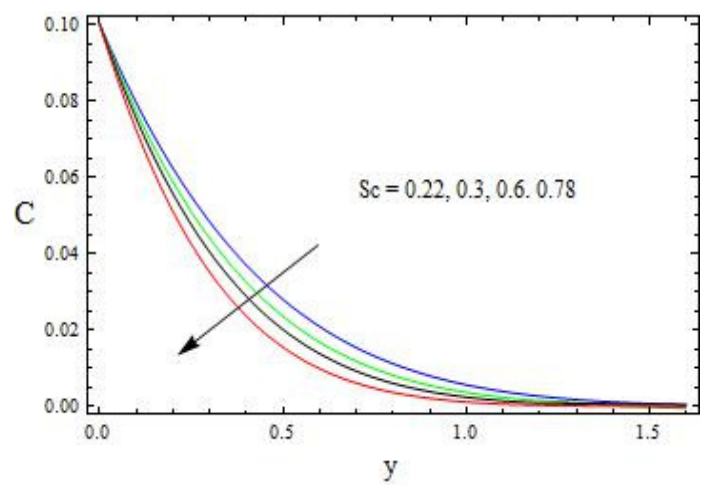


Figure 13: The Concentration Profile for C against Sc with t=0.1

Table 1: Skin friction (τ)

R	M	K	α	Pr	Gr	Gm	Sc	t	τ
1	2	1	1	0.71	3	5	2	0.2	3.82554
2									4.92588
3									5.85145
	3								3.47885
	4								2.52245
		2							4.22516
		3							5.26355
			2						6.32556
			3						8.25669
				0.16					2.22549
				3					5.62898
					4				4.25889
					5				5.36699
						8			7.58554
						10			10.9885
							3		3.96589
							4		4.52699
								0.3	4.11052
								0.4	5.68470

Table 2: The Nusselt number (Nu)

R	Pr	t	Nu
1	0.71	0.1	0.195870
2	0.71	0.1	0.216376
3	0.71	0.1	0.235839
4	0.71	0.1	0.254358
1	0.16	0.1	0.107555
1	3	0.1	0.634710
1	7	0.1	1.393160
1	0.71	0.2	0.331442
1	0.71	0.3	0.461249
1	0.71	0.4	0.588593

Table.3: The Sherwood number (Sh)

Sc	t	Sh
2	0.1	0.104512
3	0.1	0.226218
4	0.1	0.356825
5	0.1	0.493120
2	0.2	0.147802
2	0.3	0.181019
2	0.4	0.209023
2	0.5	0.233695

4. CONCLUSIONS

In this paper we study the unsteady MHD flow of visco-elastic fluid past an impulsively started vertical porous plate with variable heat and mass transfer. The following conclusions follow from the above discussion:

- 1. The velocity decreases on increasing the intensity of the magnetic field.
- 2. The velocity increases with increasing D, the permeability parameter or the visco-elastic parameter α .
- 3. The magnitude of the velocity enhances and reduces continuously with increasing the radiation parameter R.
- 4. The velocity increases with increasing time t. It is also observed that the magnitude of the velocity u decreases with increasing Prandtl number Pr.
- 5. The velocity decreases with increasing thermal Grashof number Gr (cooling plate), whereas there is a sharp enhancement in velocity on heating the plate and this is increase sustains away from the plate.
- 6. The magnitude of the velocity increases with increasing mass Grashof number Gm throughout the fluid region. The same phenomenon is observed with increasing Schmidt number *Sc*.
- 7. The temperature decreases with increasing radiation parameter R or Pr.
- 8. The increasing values of Schmidt number Sc lead to a fall in the concentration profiles throughout the fluid.
- 9. The skin friction enhances with increasing R, D, α , Pr, Gr, Gm, Sc and time t, while decreases with M and -Gr.
- 10. Nusselt number Nu increases with increasing R, Pr and t.
- 11. The Sherwood number goes on increasing with increasing *Sc* and *t*, while the Nusselt number Nu increases with increasing R, Pr and *t*.

APPENDIX:

$$\xi = \frac{y}{2\sqrt{t}}, \quad a_1 = 1 + \frac{\xi \Pr}{\sqrt{Rt}}, \quad a_2 = 1 - \frac{\xi \Pr}{\sqrt{Rt}}, \quad a_3 = \frac{R - \left(M^2 + \frac{1}{D}\right)}{1 - \Pr}, \quad a_4 = \frac{\left(M^2 + \frac{1}{D}\right)}{Sc - 1}$$

$$a_5 = \frac{1}{2} \left(a_9 + a_{10} \left(t - \frac{y}{2\sqrt{M^2 + (1/D)}}\right)\right), \quad a_6 = \frac{1}{2} \left(a_9 + a_{10} \left(t + \frac{y}{2\sqrt{M^2 + (1/D)}}\right)\right)$$

$$a_7 = \frac{a_{11}}{2} \left(1 + a_3 t - \frac{y a_3 \sqrt{\Pr}}{2\sqrt{R/\Pr}}\right), \quad a_8 = \frac{a_{11}}{2} \left(1 + a_3 t + \frac{y a_3 \sqrt{\Pr}}{2\sqrt{R/\Pr}}\right), \quad a_9 = 1 + a_{11} + a_{12},$$

$$a_{10} = \frac{Gr}{a_3 (1 - \Pr)} + \frac{Gm}{a_4 (1 - Sc)}, \quad a_{11} = \frac{Gr}{a_3^2 (1 - \Pr)}, \quad a_{12} = \frac{Gm}{a_4^2 (1 - Sc)}$$

NOMENCLATURE

Volumetric coefficient of thermal expansion			Thermal Grashof number		
Volumetric coefficient of expansion with			Darcy parameter		
concentration			is the normal stress modulus,		
σ	Stefan-Boltzmann constant	k	Thermal conductivity of the fluid		
ρ	Density	M	Magnetic field parameter		
θ	Dimensionless temperature	Nu	Dimensional Nusselt number		
ν	Kinematic viscosity	Pr	Prandtl number		
μ	Coefficient of viscosity	q_r	Radiative heat flux in the y direction		
τ	Dimensionless skin friction	R	Radiation parameter		
-		Sc	Schmidt number		
$b_{_{_{\boldsymbol{y}}}}$	Similarity parameter	Sh	Dimensional Sherwood number		
a*	Absorption coefficient	T	Temperature of the fluid near the plate		
A	Constant	t	Time		
B_0	External magnetic field		Dimensional time		
<u>C</u>	Species concentration in the fluid	T_w	Temperature of the fluid		
\overline{C}	Dimensionless concentration		Temperature of the fluid far away from the plate		
Cp	Specific heat at constant pressure	и	Velocity of the fluid in the <i>x</i> - direction		
C_w	Concentration of the fluid	u_0	Velocity of the fluid		
Concentration in the fluid far away from the			Dimensionless velocity		
plate		u y	Coordinate axis normal to the plate		
D_1	Chemical molecular diffusivity				
erf	Error function		Dimensionless coordinate axis normal to the plate		
erfc	Complementary error function	Subscripts			
g	Acceleration due to gravity	W	Conditions on the wall		
Gm	Mass Grashof number	∞	Free stream conditions		

REFERENCES

- [1]. Raptis, A. (1983). Unsteady Free Convection Flow Through a Porous Medium, *Intl. J. Eng. Sci.*, vol.21, No. 4, 345-349.
- [2]. Raptis, A. and Perdikis, P.C. (1985). Unsteady Flow Through a Porous Medium in the Presence of Free Convection. *Intl. Comm. Heat Mass Trans.*, Vol.12, 697-704.
- [3]. Sattar, M.A. (1992). Free and Forced Convection Flow Through a Porous Medium Near the Leading Edge, *Astrophys. Space Sci.*, Vol.191, 323-328.
- [4]. Singh, A.K. and Dikshit, C.K. (1988). Hydromagnetic Flow Past a Continuously Moving Semi-Infinite Plate for Large Suction, *Astrophys. Space Sci.*, Vol.148, 249-256.
- [5]. Veera Krishna M. and Gangadhar Reddy M. (2016). MHD free convective rotating flow of viscoelastic fluid past an infinite vertical oscillating porous plate with chemical reaction," IOP Conf. Series: Materials Science and Engineering 149, 012217, doi: http://dx.doi.org/10.1088/1757-899X/149/1/012217.
- [6]. Veera Krishna M. and Subba Reddy G. (2016). Unsteady MHD convective flow of second grade fluid through a porous medium in a rotating parallel plate channel with temperature dependent source, *IOP Conf. Series: Materials Science and Engineering*, 149, 012216, doi: http://dx.doi.org/10.1088/1757-899X/149/1/012216.
- [7]. Veera Krishna M. and Swarnalathamma B.V. (2016). Convective Heat and Mass Transfer on MHD Peristaltic Flow of Williamson Fluid with the Effect of Inclined Magnetic Field, *AIP Conference Proceedings*, 1728, 020461,doi: http://dx.doi.org/10.1063/1.4946512
- [8]. Swarnalathamma B. V. and Veera Krishna M. (2016). Peristaltic hemodynamic flow of couple stress fluid through a porous medium under the influence of magnetic field with slip effect, *AIP Conference Proceedings*, 1728, 020603, doi: http://dx.doi.org/10.1063/1.4946654
- [9]. Krishna, D.V., Siva Prasad, R. and Veera Krishna, M. (2009). Unsteady Hydro Magnetic Flow of an Incompressible Viscous Fluid in a Rotating Parallel Plate Channel with Porous Lining, *Journal of Pure and Applied Physics*, 21, 131-137.

- [10]. Veera Krishna, M., Suneetha, S.V. and Siva Prasad, R. (2010). Hall Effects on Unsteady Hydro Magnetic Flow of an Incompressible Viscous Fluid in a Rotating Parallel Plate Channel with Porous Lining, *Journal of Ultra Scientist of Physical Sciences*, 22, 95-106.
- [11]. Veera Krishna, M., Suneetha, S.V. and Siva Prasad, R. (2009). Steady Hydro Magnetic Flow of a Couple Stress Fluid through a Composite Medium in a Rotating Parallel Plate Channel with Porous Bed on the Lower Half, *Proceedings of 54th Congress of Indian Society of Theoretical and Applied Mechanics*, New Delhi, 18-21 December 2009, 140-149.
- [12]. Veera Krishna, M., Siva Prasad, R. and Krishna, D.V. (2010). Hall Effects on Steady Hydro Magnetic Flow of a Couple Stress Fluid through a Composite Medium in a Rotating Parallel Plate Channel with Porous Bed on the Lower Half, *Advanced Studies in Contemporary Mathematics*, 20, 457-468.
- [13]. Veera Krishna, M. and Malashetty, S.G. (2012). Unsteady Flow of an Incompressible Electrically Conducting Second Grade Fluid through a Porous Medium in a Rotating Parallel Plate Channel Bounded by a Porous Bed, *International Journal of Applied Mathematics and Mechanics*, 8, 61-84.
- [14]. Veera Krishna, M. and Malashetty, S.G. (2011). Hall Effects on Unsteady Flow of an Incompressible Electrically Conducting Second Grade Fluid through a Porous Medium in a Rotating Parallel Plate Channel Bounded by a Porous Bed, *International Journal of Advances in Science and Technology*, 2, 87-102.
- [15]. Veera Krishna, M., Subba Reddy, G. and Chamkha, A.J. (2018). Hall effects on unsteady MHD oscillatory free convective flow of second grade fluid through porous medium between two vertical plates, *Physics of Fluids*, 30, 023106,doi: https://doi.org/10.1063/1.5010863
- [16]. Veera Krishna, M. and Chamkha, A.J. (2018). Hall effects on unsteady MHD flow of second grade fluid through porous medium with ramped wall temperature and ramped surface concentration, Physics of Fluids, 30, 053101 (2018), doi: https://doi.org/10.1063/1.5025542
- [17]. Veera Krishna, M., Gangadhara Reddy, M. and Chamkha, A.J. (2019), Heat and Mass Transfer on MHD Rotating Flow of Second Grade Fluid Past an Infinite Vertical Plate Embedded in Uniform Porous Medium with Hall Effects, *Applied Mathematics and Scientific Computing*, *Trends in Mathematics*, 417-427, doi: https://doi.org/10.1007/978-3-030-01123-9_41.